Performance Analysis of Latent Heat Storage Systems using CuO Nanoparticles

Dawit Gudeta Gunjo
Department of Mechanical Engineering, Adama Science and Technology University

Vinod Kumar Yadav
Department of Mechanical Engineering, G. L. Bajaj Institute of Technology and Management

Devendra Kumar Sinha
Department of Mechanical Design and Manufacturing Engineering, Adama Science and Technology University

https://doi.org/10.5109/4793667

出版情報：Evergreen. 9 (2), pp.292-299, 2022-06. Transdisciplinary Research and Education Center for Green Technologies, Kyushu University
バージョン：

Performance Analysis of Latent Heat Storage Systems using CuO Nanoparticles

Dawit Gudeta Gunjo[1], Vinod Kumar Yadav[2,*] Devendra Kumar Sinha[3]

[1]Department of Mechanical Engineering, Adama Science and Technology University, Adama Ethiopia,

[2]Department of Mechanical Engineering, G. L. Bajaj Institute of Technology and Management, Greater N oida, India

[3]Department of Mechanical Design and Manufacturing Engineering, Adama Science and Technology Univ ersity, Ethiopia

*Author to whom correspondence should be addressed:
E-mail: vinod.yadav@glbitm.ac.in

(Received February 17, 2022; Revised May 1, 2022; accepted May 5, 2022).

Abstract: The quality of phase change material (PCM) employed determines the thermal behavior of latent heat storage systems (LHSS). In this paper, the behavioral aspects, related to the storage characteristics of PCMs, are evaluated numerically using COMSOL Multiphysics®4.3a software. Experiments are also conducted to validate the numerical results. Paraffin-based nanofluid seeded with 4% copper oxide (CuO) nanoparticles, as phase changing material, is studied to evaluate the effect of nanoparticles addition on the storage qualities of the LHSS. It was observed that with 4% CuO nanoparticle seeding, the rate of melting and solidification get enhanced by 1.7 times and 1.8 times respectively compared to pure paraffin-filled LHSS. It was observed that with addition of 4% CuO nanoparticles, the density, viscosity and thermal conductivities is increased by about 29%, 18.3%, 55% respectively compared to base material (i.e., pure paraffin). However, the latent and sensible heats get reduced by 26% and 18.5% respectively. In addition, seeding of CuO reduces the charging time by 70% compared to the LHSS based on pure paraffin.

Keywords: Dispersion, CuO nanoparticles, Latent heat storage, Melt fraction

1. Introduction

India is enriched with vast solar energy potential. Still, the storage of energy, recovered from the sun, is a challenge due to its intermittent supply. There is a strong need of development of thermal storage systems, capable of storing significant amount of energy exploited from the sun. Latent Heat Storage Systems (LHSS) are becoming popular these days in solar thermal storing applications.

Kalogirou[1)] and Bouhal et al.[2)] evaluated the life cycles of flat plate collectors and reported them to be one of the promising and cost-effective devices that produce no harm to the environment. Keyanpour et al.[3)] investigated the applications and economics of heating systems based on solar using TRNSYS program[4,5)]. Gunjo et al.[6,7)] conducted experiments and numerical simulations to study the effect of different operating parameters on the thermal efficiency and exit water temperature of solar water heating systems. They reported that to remove the barrier of intermittency of the solar energy, the thermal energy storage systems are one of the viable solutions. Compared to the sensible heat storage systems, the latent heat storage technologies are more promising owing to their superior storage, high energy density, better heat of fusion, and economy[8)]. LHSS employs phase change materials (PCMs) to store and exhale a good amount of energy, as heat, at any given temperature, and hence mends the gap between the supply and the demand of energy.

Fan and Khodadadi[9-11)] evaluated and provided the strategies for maximizing the conductivity of PCMs seeded with nanoparticles. Farid et al.[12)] summarized the benefits of using paraffin wax for a larger range of high and low temperature utilization. Jesumathy et al.[13)] studied the performance characteristics of LHSS based on paraffin-wax and observed that the HTF's inlet temperature reduces the melting time of the systems. Agarwal and Sarviya[14)] evaluated the efficacy of LHSS based on the paraffin-wax for solar drying applications utilizing water as the HTF. Rabha and Muthukumar[15)] studied the solar drier's performance with paraffin wax and reported an improvement in the performance even during off-peak hours of sun's availability. Kabeel et al.[16,

[17] reported that the LHSS produces more fresh water. In addition, using solar heating system, with flat plate, and paraffin wax filled LHS, the daily efficiency improves significantly. Salunkhe and Krishna[18] also reported that the use of paraffin wax is a good choice for water heating applications in which the sun acts as heat source. Niyas et al.[19] performed computational analysis of LHS based on paraffin wax and reported it to be superior technology compared to conventional systems.

Khodadadi and Hosseinizadeh[20] and Nabil and Khodadadi[21] reported that nanoparticle dispersion improves the thermal characteristics of PCMs by enhancing thermal conductivity and heat release rate of the base materials. Zabalegui et al.[22] investigated the behaviour of nanofluids based on paraffin over carbon nanotubes, with multiple layers, and revealed a reduction in latent heat and increase in thermal conductivity. Dheep and Sreekumar[23] reported that carbon-based nanofluids are superior in phase change characteristics compared to other materials. Khanafer et al.[24] performed a numerical investigation of the heat transfer characteristics of nanofluids and created effective conductivity maps. Thapa et al.[25] investigated an energy storage devices at small scale and observed that by adding metallic inserts and copper foams, the conductivity of the wax gets augmented. Owolabi et al.[26] explored the effect of adding iron nanoparticles on TES for solar water heating based applications and reported that addition of iron nanoparticles enhances the efficiency by about 10% thereby saving about 28.5% of annual cost. Mahian et al.[27] did the literature review of nanofluids suitable for solar thermal applications and found it to be a viable solution compared to conventional materials. Said et al.[28] studied the influence of Al_2O_3 nanoparticles on the storage capabilities. They found that 73.7% efficiency can be obtained with 13 nm particle size. Xie et al.[29-30] investigated the thermal characteristics of Al_2O_3 nanoparticles for different volume fractions. They observed that the thermal conductivity increases significantly with an increase in the fraction of volume. Xuan et al.[31-32] studied the thermal behaviour of nanofluids added with nanoparticles of copper and reported an improvement in the properties. Murshed et al.[33] investigated the conductivity of nanofluids spread with TiO_2 and found that with an increase in the volume fraction of the dispersed particle, the thermal conductivity improves.

2. Materials and method

In this paper, to improve the heat storage characteristics of solar based systems, utilizing LHS, CuO nanoparticle dispersion is used to enhance the thermal performance of the PCMs. A 5 MJ LHSS for solar heating application is developed and studied numerically and experimentally. A three-dimensional model of LHSS filled with paraffin wax was prepared and the properties were evaluated. To augment the system's performance, 4% CuO nanoparticles were also added. Shell and tube type heat exchanger (Shell dia. 300 mm, length 1000 mm, tube internal dia. 3 mm and radial thickness of 12 mm), identical to the work carried by the main author (Dawit Gudeta Gunjo) in his paper[34] is followed. The main author of this paper (Dawit Gudeta Gunjo) developed this model and experimental facility at IIT Guwahati as a part of his doctoral research. The three-dimensional domain, mesh and grid independence test report can be referred from Dawit et al.[34]. As reported, the optimum number of tubes were limited to 17. As per the findings of references[35-36], the volume fraction of the nanoparticles of CuO was fixed to 4%. The assumptions of the model were identical to author's own work[34]. The properties of CuO and the paraffin wax are presented Table 1.

Table 1. CuO and paraffin wax properties[17, 37]

Entity	Value
Specific heat $_{np}$ (CuO)	540 J/kg K
Specific heat $_{(PCM)}$	2000 J/kg K
dia_{np}(CuO)	29×10^{-9} m
$Conductivity_{np}$(CuO)	18 W/mK
Conductivity $_{PCM}$	0.2 W/mK
$Density_{PCM}$	780 kg/m^3
$Density_{np}$(CuO)	6510 kg/m^3
L_{pcm}	168000 J/kg
T_{inlet}	333.15 Kelvin
T_{ref}	273.15 Kelvin
T_m	315.15 Kelvin
$T_{intitial}$	298.15 Kelvin
Dt	3 Kelvin
T_l	$T_m + dT$ Kelvin
T_s	$T_m - dT$ Kelvin
C_1 (CuO)	0.919 (const.)
C_2 (CuO)	22.853 (const.)

2.1 Experimental procedure

The experimental facility has an outside shell, made up of stainless steel. This shell was insulated with thermos-foam to reduce the heat loss to the surrounding environment. 23 kg paraffin was used in the shell. The details of the experimental facility and its specifications are presented by author (Dawit Gudeta Gunjo) in their own work Gunjo et al.[34] from where all relevant details can be referred. The uncertainties in measurements are presented in Table 2.

Table 2. Uncertainty

Parameter	Uncertainty and unit
Diameter measurement	± 0.006 (mm)
Measurement of temperature	± 0.2 (ºC)
Measurement of solar radiation	± 5 (W/m^2)

2.2 Model validation

The developed model is validated by comparing its results with the experimental results. Fig. 1 presents the comparison of measured and predicted results. A good agreement between the two can be seen.

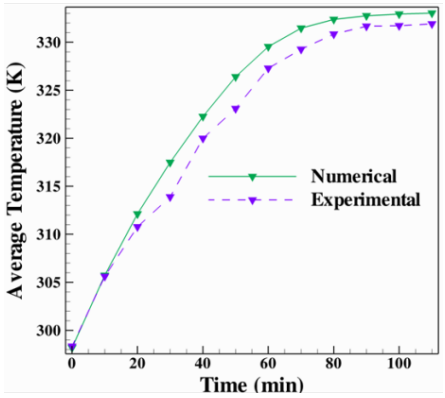

Fig. 1: Average temperature for (a) charge (b) discharge

3. Materials and method

In this work, a two dimensional model was prepared to estimate the optimized number of tubes suitable for the numerical study (Fig. 2). In this arrangement, four tubes at center and twelve tubes at the external end (Fig. 2a) and eight tubes at center and eight tubes at outer (Fig. 2b) was tested.

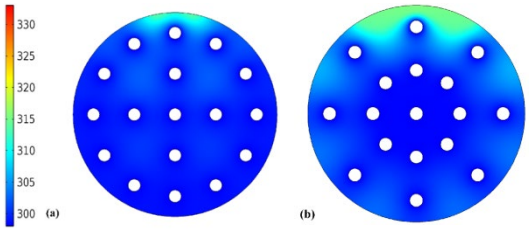

Fig. 2: Temperature distribution with (a) four inner and twelve outer tubes (b) eight inner and eight outer tubes.

The shell was maintained initially at a temperature (Ti) of 333 K and the HTF was passed though it at 298 K. After analyzing the simulated results, it was observed that the full discharge condition reached more rapidly with configuration presented in Fig. 2a compared to Fig. 2b, and hence, configuration presented in Fig. 2a is selected for analysis in the present work.

The effect of orienting the cylinder was also studied (Fig. 3a-b). It can be observed from Figures 3a-b that during first ten minutes, the melt fraction and temperature vary in similar way for horizontal as well as vertical orientations. But, after attaining melting temperature, both parameters were affected considerably thereby attaining a fully charged zone in both orientations. The maximum temperature difference of horizontal and vertical configurations was observed as 1.8 K and 3.5 K before and after melting respectively. In addition, the horizontal configuration attained full charging temperature (333 K) and a melt fraction of unity in 70 minutes. This was 20 minutes earlier than the vertical configuration. Hence, the horizontal configuration was chosen as the appropriate configuration in the present work.

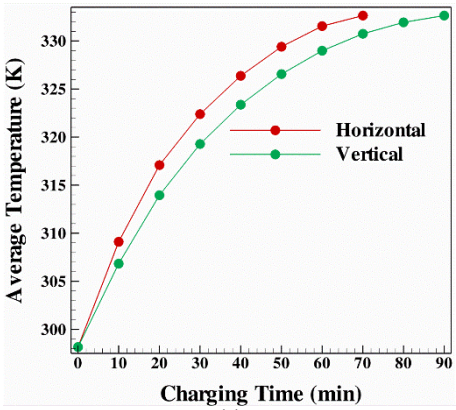

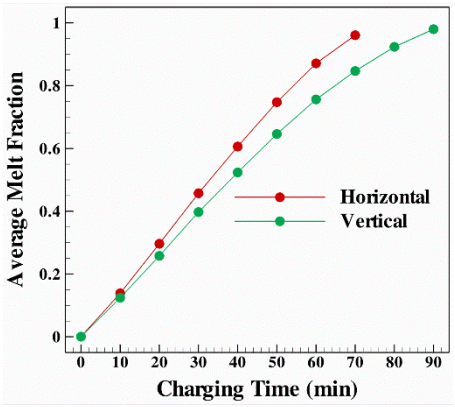

(b)

Fig. 3: Distribution of (a) temperature (b) melt fraction.

Fig. 4 depicts the contours of melt fraction during charge-discharge. The results showed that the full charge time is significantly shorter than discharge time. The nanofluid totally melts within 70 minutes, however, it took 120 minutes for solidification. The figure also shows that the whole melting of the nanofluid-filled LHS occurred within 70 minutes, and the solidification process was unfinished at that time. This is owing to the heat transfer that had occurred as a consequence of natural convection. Conversely, during discharge, conduction comes in picture due to which the charging rate is faster than discharging rate.

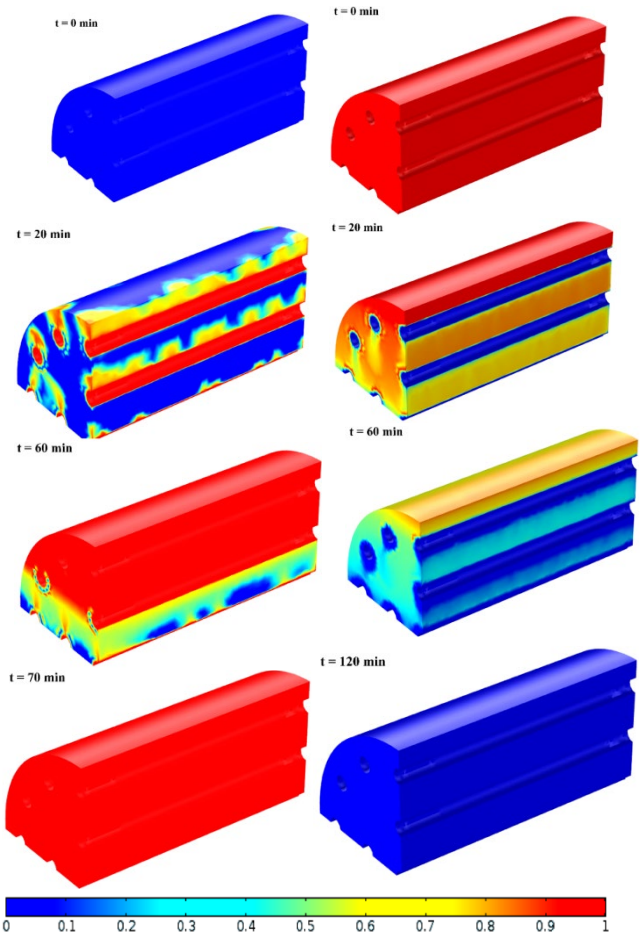

Fig. 4: Melt fraction: charge (left side) discharge (right side).

The HTF's temperature was maintained at 333 K and 298 K during the charging and discharging respectively. Figures 5a-b presents the effect of fluctuation of temperature during charging and discharging. It took 120 minutes and 70 minutes to fully charge the pure paraffin and nanofluid respectively. Hence, with CuO as a dispersed nano-fluid in paraffin, the melting rate is 1.7 times faster than pure paraffin. Fig. 5b shows that the PCM, based on pure paraffin, took 180 minutes to get fully discharged. But, the dispersed mixture took only 120 minutes, which is less by about 1.8 times.

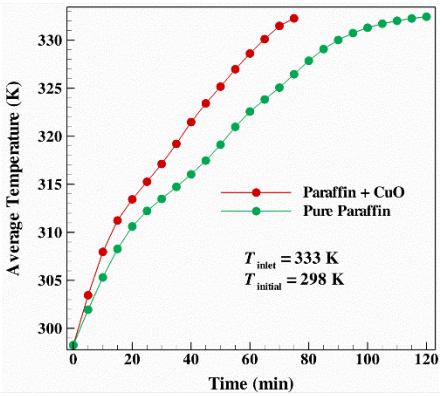

(a)

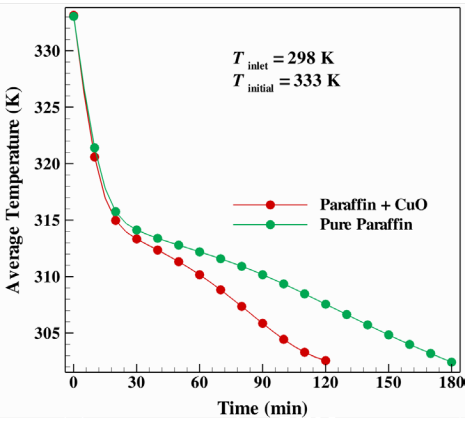

(b)

Fig. 5: Temperature (a) charge (b) discharge.

Fig. 6 depicts the time-dependent changes of average melt fraction while charge and discharge processes. During the early phase, the fraction of the melt varied slowly with the passage of time (Fig. 6a). Because the nanofluid is initially solid while charging and the primitive heat transmission occurs due to molecular diffusion. However, as time advances and phase shift comes in existence, natural convection dominates, eventually speeding up the melting process. The slope of the melt fraction with time during first phase is steeper with nanofluids compared to base material (Fig. 6a). The improvement in conductivity caused by the dispersion of highly conductive nanoparticles is one such mechanism. It is also noted that the PCM with paraffin wax fully melted in 120 minutes. On the other hand, the nanofluid melted in 70 minutes. The melting rate with nanofluid is

almost 80% faster.

Fig. 6b demonstrates that the time required to attain a fully discharged condition using nanofluid is 1.7 times faster than in paraffin wax. As the PCM is liquid in its initial phase, the buoyancy prevails and natural convection acts as the basic heat transfer mechanism. Conduction heat transfer comes in existence due to the solidification of the PCM with time. The discharge time for both nanofluids and paraffin is much longer than the charge time.

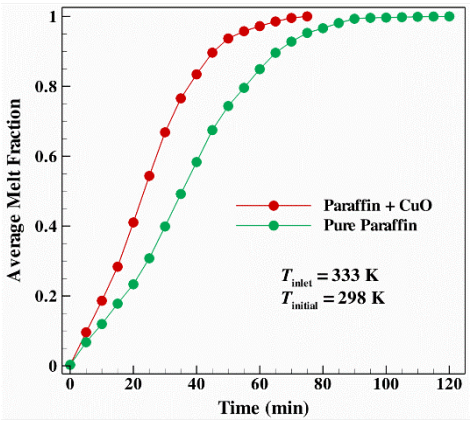

(a)

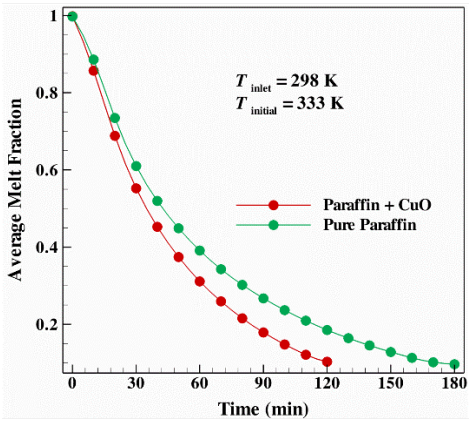

(b)

Fig. 6: Melt fraction (a) charging (b) discharge

Fig. 7 shows the deviation of various heats (sensible, latent and total). For pure paraffin and nanofluid, the highest sensible heat stored was 1.4 and 1.1 MJ respectively. Predicted data show that the nanofluid stores less sensible heat compared to paraffin. The inclusion of CuO nanoparticles lowers the specific heat of the PCM. Since, stored sensible heat vary linearly with specific heat, hence, by reducing specific heat from 2000 to 1632 J/kg K decreases the stored sensible heat. The maximum sensible heat released during discharge was observed as 1.2 and 1.4 MJ (Fig. 8) respectively.

Fig. 7 also infers that the maximum latent heat retained by the nanofluid and pure paraffin wax after reaching fully charged state is 2.8 and 3.9 MJ respectively. Although the dispersion of nanoparticles aided the speedier attainment of the charged condition, the stored latent heat of nanofluid containing CuO was significantly reduced. This is because the stored latent heat varies linearly with latent heat. In addition, the dispersion of CuO-based nanoparticles lowers the latent heat from 168 to 124.6 KJ/kg. This causes a remarkable difference in the storage of the latent heats. In the similar way, Fig. 8 shows that after attainment of completely discharged condition, the maximum heat release (latent) for paraffin and nanofluids was 3.5 and 2.6 MJ respectively. The total energy that was stored during charging was 5.4 MJ and 4.1 MJ for paraffin and nanoparticle dispersed PCM respectively. Furthermore, as plotted in Fig. 8, the heat released while discharge is 3.75 and 4.9 MJ for paraffin and nanofluids respectively.

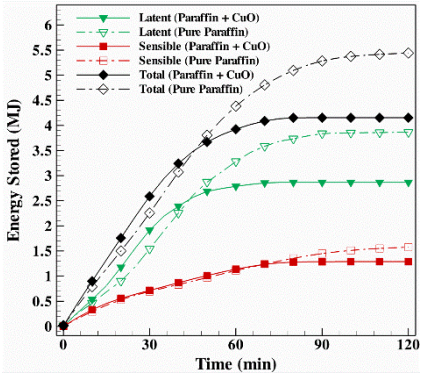

Fig. 7: Energy variation during charge

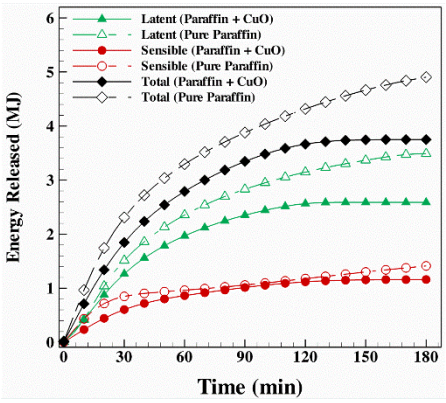

Fig. 8: Energy variation during discharge

From Fig. 9a, it can be inferred that the density do not change significantly with temperature. Rather, it increased from 760 to 980 kg/m^3 due to the addition of CuO nanoparticle (4%) in paraffin. In addition, when paraffin is dispersed with CuO nanoparticles, the viscosity and thermal conductivity increased from 0.003 Pa.s and 0.2 W/m.K to 0.0085 Pa.s and 0.31 W/m.K respectively (Fig. 9b-c). However, the trends of Fig. 9d-e indicate that latent and specific heats do not depend on temperature. The latent heat decreases from 168 to 124.6 KJ/ kg with 4% CuO addition. The specific heat dropped from 2000 to 1632 J/ kg K. This was due to the decrease

in heat of fusion and heat capacity.

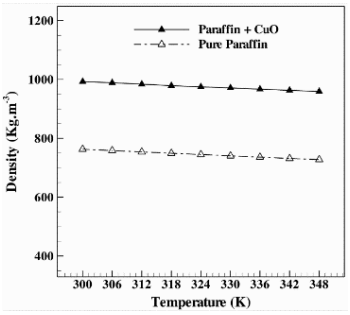

(a)

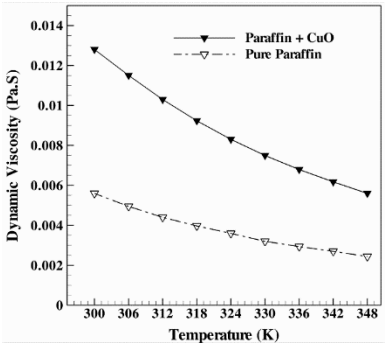

(b)

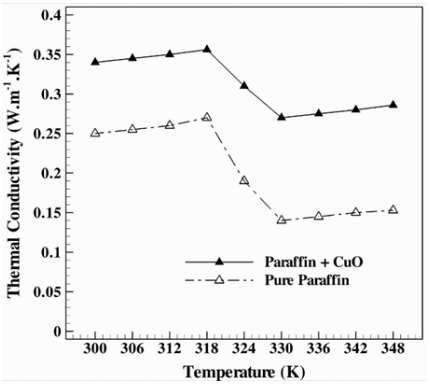

(c)

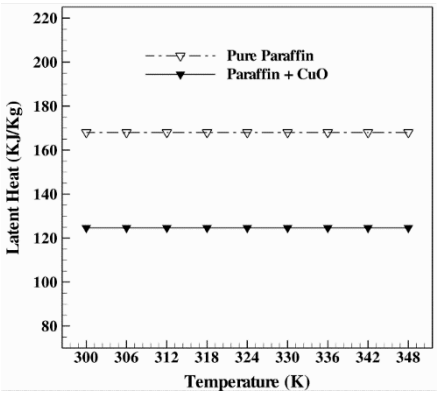

(d)

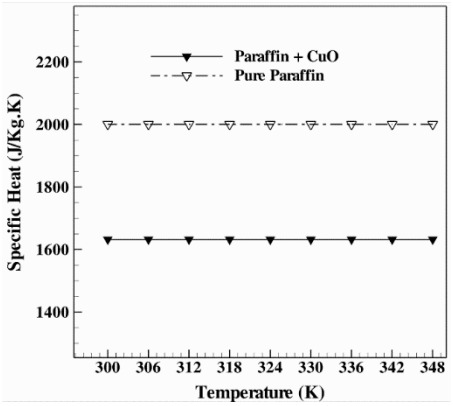

(e)

Fig. 9: Parameters variation with temperature (K) (a) density, (b) viscosity (c) conductivity, (d) latent heat (LH) and (e) specific heat.

The results plotted in Figure 9 infers that with addition of 4% CuO nanoparticles, the density, viscosity and thermal conductivities is increased by about 29%, 18.3%, 55% respectively compared to base material. However, the latent and sensible heats get reduced by 26% and 18.5% respectively. This clearly indicates that most of the thermal properties get enhanced by the addition of CuO nanoparticles.

4. Conclusions

In this paper, numerical examination, using 3D model of heat exchanger (shell and tube) containing LHS was performed. The computed results of pure paraffin and 4% CuO-dispersed-paraffin were compared with experiments and a fair agreement was noticed. It was observed that in the case of nanofluid, the time required to attain a totally charged state less by about 70% compared to base paraffin-based LHS. In addition, with nanoparticles, the time required for attaining a discharge state was approximately 1.8 times faster compared to base material. The key findings of this work are summarized as:

1. With dispersion of 4% CuO nanoparticles, the specific heat gets reduced, resulting in a 0.3 MJ and 0.2 MJ decrease in net sensible heat storage and release during the charge and discharge process respectively compared to pure paraffin.
2. Because of the reduction in heat of fusion during the charge/discharge, the latent heat storage/release by the nanofluid gets reduced by 1.1 MJ to 0.9 MJ compared to LHS filled with paraffin.
3. The addition of 4% CuO nanoparticles to paraffin decreased the latent as well as specific heat of original fluid while it increases the viscosity, conductivity, and density. The studies[38-43] presents the approaches that deal with energy relevant to various fields.

Acknowledgements

This work was conducted by Dawit Gudeta Gunjo in IIT Guwahati while pursuing his doctoral research.

References

1) S. Kalogirou, "Thermal performance, economic and environmental life cycle analysis of thermosiphon solar water heaters," Solar Energy., 83(1) 39-48 (2009).
2) T. Bouhal, Y. Agrouaz, A. Allouhi, T. Kousksou, A. Jamil, T. El Rhafiki, Y. Zeraouli, "Impact of load profile and collector technology on the fractional savings of solar domestic water heaters under various climatic conditions," International Journal of Hydrogen Energy., 42(18) 13245-13258 (2017).
3) M. Keyanpour-Rad, H.R. Haghgou, F. Bahar, E. Afshari, "Feasibility study of the application of solar heating systems in Iran," Renewable Energy., 20(3) 333-345 (2000).
4) S.A. Kalogirou, "Flat-plate collector construction and system configuration to optimize the thermosiphonic effect," Renewable Energy., 67 202-206 (2014).
5) S.A. Kalogirou and C. Papamarcou, "Modelling of a thermosyphon solar water heating system and simple model validation," Renewable Energy., 21(3-4) 471-493 (2000).
6) D.G. Gunjo, P Mahanta, P.S. Robi, "CFD and experimental investigation of flat plate solar water heating system under steady state condition," Renewable Energy., 106 24-36 (2016).
7) D.G. Gunjo, P. Mahanta, P.S. Robi, "Exergy and energy analysis of a novel type solar collector under steady state condition: Experimental and CFD," Renewable Energy., 114 655-669 (2017).
8) A. Sharma, V.V. Tyagi, C.R. Chen, D. Buddhi, "Review on thermal energy storage with phase change materials and applications," Renewable and Sustainable Energy Reviews., 13(2) 318-345 (2009).
9) L. Fan and J.M. Khodadadi, "Thermal conductivity enhancement of phase change materials for thermal energy storage: A review," Renewable and Sustainable Energy Reviews., 15(1) 24-46 (2011).
10) L. Fan and J.M. Khodadadi, "A theoretical and experimental investigation of unidirectional freezing of nanoparticle-enhanced phase change materials. Transactions of the ASME," Journal of Heat Transfer., 134(9) 092301(1-9) (2012).
11) L. Fan and J.M. Khodadadi, "An experimental investigation of enhanced thermal conductivity and expedited unidirectional freezing of cyclohexane-based nanoparticle suspensions utilized as nano-enhanced phase change materials (NePCM)," International Journal of Thermal Sciences., 62 120-126 (2012).
12) M.M. Farid, A.M. Khudhair, S.A.K. Razack, S. Al-Hallaj, "A review on phase change energy storage: materials and applications," Energy Conversion and Management, 45 1597-1615 (2004).
13) S.P. Jesumathy, M. Udaykumar, S. Suresh, S. Jegadheeswaran, "An experimental study on heat transfer characteristics of paraffin wax in horizontal double pipe heat latent heat storage unit," Journal of the Taiwan Institute of the Chemical Engineers., 45(4) 1298-1306 (2014).
14) A. Agarwal and R.M. Sarviya, "An experimental investigation of shell and tube latent heat storage for solar dryer using paraffin wax as heat storage material," Engineering Science and Technology, an International Journal., 19(1) 619-631 (2016).
15) D.K. Rabha and P. Muthukumar, "Performance studies on a forced convection solar dryer integrated with a paraffin wax–based latent heat storage system," Solar Energy., 149 214-226 (2017).
16) A.E. Kabeel, M. Elkelawy, H.A.E. Din, A. Alghrubah, "Investigation of exergy and yield of a passive solar water desalination system with a parabolic concentrator incorporated with latent heat storage medium," Energy Conversion and Management., 145 10-19 (2017).
17) A.E. Kabeel, A. Khalil, S.M Shalaby, M.E. Zayed, "Improvement of thermal performance of the finned plate solar air heater by using latent heat thermal storage," Applied Thermal Engineering., 123 546-553 (2017).
18) P.B. Salunkhe and D.J. Krishna, "Investigations on latent heat storage materials for solar water and space heating applications," Journal of Energy Storage., 12 243-260 (2017).
19) H. Niyas, S. Prasad, P. Muthukumar, "Performance investigation of a lab-scale heat storage prototype – Numerical results," Energy Conversion and Management., 135 188-199 (2017).
20) J.M. Khidadadi and S.F. Hosseinizadeh, "Nanoparticle-enhanced phase change materials (NEPCM) with great potential for improved thermal energy storage," International Communications in Heat and Mass Transfer., 34(5) 534-543 (2007).
21) M. Nabil and J.M. Khodadadi, "Experimental determination of temperature-dependent thermal conductivity of solid eicosane-based nanostructure-enhanced phase change materials," International Journal of Heat and Mass Transfer., 67 301-310 (2013).
22) A. Zabalegui D. Lokapur, H. Lee, "Nanofluid PCMs for thermal energy storage: Latent heat reduction mechanisms and a numerical study of effective thermal storage performance," International Journal of Heat and Mass Transfer., 78 1145-1154 (2014).
23) G.R. Dheep and A. Sreekumar, "Influence of nanomaterials on properties of latent heat solar

thermal energy storage materials," Energy Conversion and Management., 83 133-148 (2014).
24) K. Khanafer, K. Vafai, M. Lightstone, "Buoyancy-driven heat transfer enhancement in a two-dimensional enclosure utilizing nanofluids," International Journal of Heat and Mass Transfer., 46 3639-3653 (2003).
25) Thapa, S., Chukwu, S., Khaliq, A. and Weiss, L., "Fabrication and analysis of small-scale thermal energy storage with conductivity enhancement," Energy Conversion and Management., 79 161-170 (2014).
26) O. Mahian, A. Kianifar, S.A. Kalogirou, I. Pop, S. Wongwises, "A review of the applications of nanofluids in solar energy," International Journal of Heat and Mass Transfer., 57(2) 582-594 (2013).
27) A.L. Owolabi, H.H. Al-Kayiem, A.T. Baheta, "Performance investigation on a thermal energy storage integrated solar collector system using nanofluid," International Journal of Energy Research., 41(5) 650-657 (2017).
28) Z. Said, R. Sidur, N.A. Rahim, "Energy and exergy analysis of a flat plate solar collector using different sizes of aluminium oxide based nanofluid," Journal of Cleaner Production., 133 518-530 (2016).
29) H. Xie, J. Wang, T. Xi, Y. Liu, F.A. Wu, "Thermal conductivity enhancement of suspensions containing nanosized alumina particles," Journal of Applied Physics., 91(7) 4568-4572 (2002).
30) H. Xie, J. Wang, T. Xi, Y. Liu, "Thermal conductivity of suspensions containing nanosized," International Journal of Thermophysics., 23(2) 571-580 (2002).
31) Y. Xuan and Q. Li, "Heat transfer enhancement of nanofluids," International Journal of Heat and Fluid Flow., 21(1) 58-64 (2000).
32) Y. Xuan, Q. Li, W. Hu, "Aggregation structure and thermal conductivity of nanofluids," AlChE Journal., 49(4) 1038-1043 (2000).
33) S.M. S. Murshed, K.C. Leong, C. Yang, "Enhanced thermal conductivity of TiO_2 –water based nanofluids," International Journal of Thermal Sciences., 44 367-373 (2005).
34) G. G. Dawit, S. R Jena, P Mahanta, P.S. Robi, "Melting enhancement of a latent heat storage with dispersed Cu, CuO and Al_2O_3 nanoparticles for solar thermal application," Renewable Energy., 121, 652-665 (2018).
35) R.S. Vajjha and D.K. Das, "Experimental determination of thermal conductivity of three nanofluids and development of new correlations," International Journal of Heat and Mass Transfer., 52 4675-4682 (2009).
36) R.S. Vajjha, D.K. Das, P.K. Namburu, "Numerical study of fluid dynamic and heat transfer performance of Al_2O_3 and CuO nanofluids in the flat tubes of a radiator," International Journal of Heat and Fluid Flow., 31 613-621 (2010).
37) A.P. Sasmito, J.C. Kurnia, A.S. Mujumdar, "Numerical evaluation of laminar heat transfer enhancement in nanofluid flow in coiled square tubes," Nanoscale Research Letters., 6(1) 376-390 (2011).
38) A.S. Syahrul, J.T. Oh, N. Mohd-Ghazali, A. Robiah, and Y. Mohd-Yunos, "Entropy Generation Minimization of Two-Phase Flow in a Mini Channel with Genetic Algorithm," Evergreen, 6 (1) 39-43 (2019). doi:10.5109/2321004.
39) N. Hamzah, M.F. Mohd Yasin, M.Z. M. Yusop, and M.T. Zainal, "Identification of CNT Growth Region and Optimum Time for Catalyst Oxidation: Experimental and Modelling Studies of Flame Synthesis," Evergreen, 6 (1) 85-91 (2019). doi:10.5109/2328409.
40) M. Barai, and B. Saha, "Energy Security and Sustainability in Japan," Evergreen Joint J Nov Carbon Resource Science Green Asia Strategy, 2 (1) 49-56 (2015). doi:10.5109/1500427.
41) M.I. Hamid, N. Nasruddin, Budihardjo, and E. Susanto, "Refrigeration Cycle Exergy-Based Analysis of Hydrocarbon (R600a) Refrigerant for Optimization of Household Refrigerator," Evergreen, 6 (1) 71-77 (2019). doi: 10.5109/2321015.
42) Y.D. Kim, K. Thu, and C.N. Kim, "Evaluation and Parametric Optimization of the Thermal Performance and Cost Effectiveness of Active-Indirect Solar Hot Water Plants," Evergreen, 2 (2) 50-60 (2015). doi:10.5109/1544080.
43) H. Gima, and T. Yoshitake, "A comparative study of energy security in okinawa prefecture and the state of hawaii," Evergreen, 3 (2) 36–44 (2016). doi:10.5109/1800870.